View metadata, citation and similar papers at core.ac.uk
brought to you by CORE
provided by Publications of the IAS Fellows

J Mater Sci: Mater Electron (2010) 21:355–359
DOI 10.1007/s10854-009-9920-5

ZnO nanocrystalline thin films: a correlation of microstructural, optoelectronic properties

V. B. Patil · S. G. Pawar · S. L. Patil · S. B. Krupanidhi

Received: 27 March 2009 / Accepted: 19 May 2009 / Published online: 6 June 2009
© Springer Science+Business Media, LLC 2009

Abstract The compositional, structural, microstructural, dc electrical conductivity and optical properties of undoped zinc oxide films prepared by the sol–gel process using a spin-coating technique were investigated. The ZnO films were obtained by 5 cycle spin-coated and dried zinc oxide films followed by annealing in air at 600 °C. The films deposited on the platinum coated silicon substrate were crystallized in a hexagonal wurtzite form. The energy-dispersive X-ray (EDX) spectrometry shows Zn and O elements in the products with an approximate molar ratio. TEM image of ZnO thin film shows that a grain of about 60–80 nm in size is really an aggregate of many small crystallites of around 10–20 nm. Electron diffraction pattern shows that the ZnO films exhibited hexagonal structure. The SEM micrograph showed that the films consist in nanocrystalline grains randomly distributed with voids in different regions. The dc conductivity found in the range of 10^{-5}–10^{-6} $(\Omega\ \mathrm{cm})^{-1}$. The optical study showed that the spectra for all samples give the transparency in the visible range.

1 Introduction

As an important semiconductor material, ZnO has been used widely for its optical, electrical, optoelectronic, catalytic and photochemical properties, including optical waveguides [1, 2], transparent conducting coatings [3] and catalysis, etc. [4]. Its wide band gap of 3.37 eV at room temperature is also suitable for photoelectronic materials in the blue-ultraviolet region [5]. For the wide variety of applications, numerous ZnO film preparation methods have been attempted: r.f. and magnetron sputtering [1–3, 8, 9], spray pyrolysis [10–13], chemical vapor deposition CVD [14–18], and the sol gel process [19]. Recently pulsed laser deposition [20, 21] was reported for ZnO film fabrication. The electrical conduction of ZnO films at temperatures above room temperature has been understood to be thermal excitation of electrons from donor levels originated by defects or impurity atoms. In polycrystalline ZnO films deposited by CVD [18], electronic conduction around room-temperature has been attributed to band transport involving thermionic and thermal field emission over grain boundaries in the films. Zinc oxide films deposited by chemical spray pyrolysis had resistivity approximately $\approx 10^{-3}\ \Omega$ cm [4]. Al-doped ZnO films formed by sol–gel dip coating gave resistivities of (7–10) $\times\ 10^{-4}\Omega$ cm [19].

In this work, we shall deal with compositional, microstructural, electrical and optical properties of ZnO thin films prepared by the sol–gel process.

2 Experimental details

ZnO thin films were prepared by the sol–gel method. As a starting material, zinc acetate dihydrate $(Zn\ (CH_3CO_2)_2 \cdot 2H_2O)$ and RG grade methanol was used. The resultant solution was stirred at 60 °C for 30 min to yield a clear and homogeneous solution, which served as the coating solution. A solution of ZnO precursor was deposited on a Platinum coated Silicon substrate by a single wafer spin processor (Lawrell Technology Corporation, Model WS-500-6NPP/LITE). After setting the substrate on the disk of the spin

V. B. Patil (✉) · S. G. Pawar · S. L. Patil
Department of Physics, Solapur University, Solapur, M.S, India
e-mail: drvbpatil@gmail.com

S. B. Krupanidhi
Materials Research Centre, Indian Institute of Science, Bangalore, India

coater, the coating solution approximately 0.2 ml was dropped and spin-coated with 4,000 rev. min^{-1} for 40 s in air. Figure 1 shows the flow diagram for ZnO films prepared from the sol–gel process using the spin-coating method.

The structural properties of the films were investigated by X-ray diffraction (XRD) (Philips PW-3710, Holland) using filtered Cu Kα radiation ($\lambda = 1.54056$ Å). High resolution Transmission electron microscopy (HRTEM) images were taken with a Hitachi Model H-800 transmission electron microscope. Energy-dispersive X-ray analyses were recorded on a JEOL-2010 TEM. The surface morphologies of the films were observed by scanning electron microscopy (SEM) using a Quanta-200, Holland. The thickness of the film was determined using cross section of SEM.

The electrical characterization was performed on the sample in the MIS (Metal–Insulator–Semiconductor) configuration. The optical absorption spectra of ZnO thin films were measured using a double-beam spectrophotometer Shimadzu UV-140 in the 300–1,000 nm-wavelength range.

3 Results and discussion

3.1 Structural studies

Figure 2 shows the X-ray diffraction patterns of as grown and annealed films at different temperatures. The effect of annealing temperature on the crystallinity of ZnO thin films can be understood from the figure. The annealing temperature was varied from 400 to 600 °C with a fixed annealing time of 30 min.

The X-ray spectra show well-defined diffraction peaks showing good crystallinity. The crystallites are randomly oriented and the d-values calculated for the diffraction peaks are in good agreement with those given in JCPD data card (79.0208) for ZnO. This means that ZnO has been crystallized in a hexagonal wurtzite form. The lattice constants calculated from the present data are $a = 3.235$ Å and $c = 5.181$Å respectively. From Fig. 2 it is seen that the (002) peak intensity increased with an increase in the annealing temperature. However, the full width at half-maxima FWHM of the (002) peaks was hardly changed with increasing film annealing temperature. The grain size of all ZnO samples annealed at 400–600 °C was calculated and it is in the range of 50–110 nm from the XRD peaks using Scherrer's equation revealing a fine nanocrystalline grain structure.

3.2 Microstructural studies

The energy-dispersive X-ray (EDX) spectrometry shown in Fig. 3 clearly shows Zn and O elements in the products with an approximate molar ratio of 1:1 (the Cu signal is attributed to the copper meshes for TEM).

Figure 4a shows TEM image of ZnO thin film annealed at 600 °C. It clearly shows that a grain of about 60–80 nm in size is really aggregate of many small crystallites of

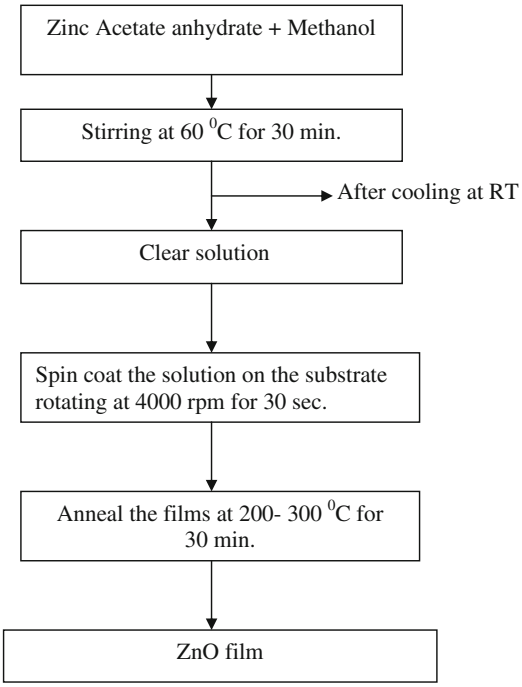

Fig. 1 Flow diagram for ZnO films prepared from the sol–gel process using the spin-coating method

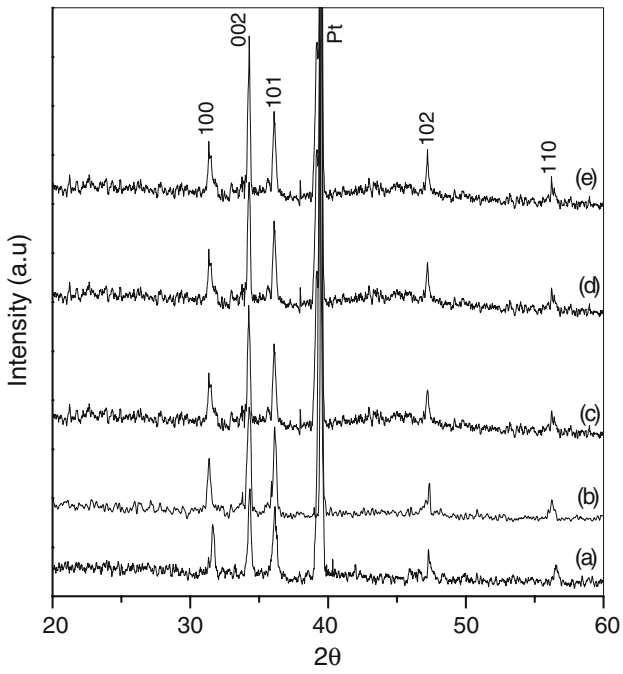

Fig. 2 X ray diffractograms of ZnO thin films at different annealing temperatures: **a** 400 °C, **b** 450 °C, **c** 500 °C, **d** 550 °C and **e** 600 °C

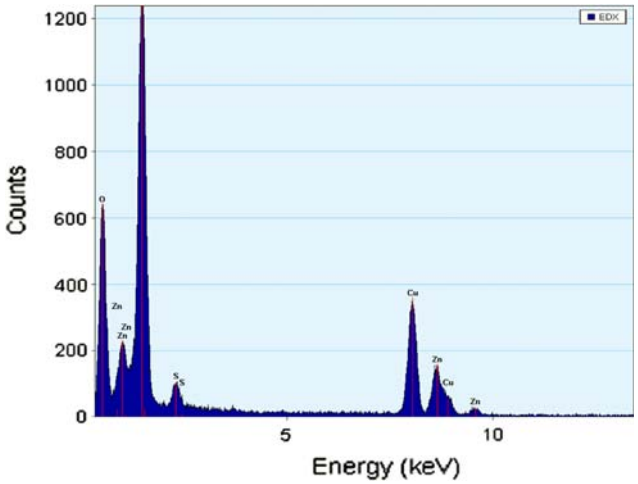

Fig. 3 The energy-dispersive X-ray (EDX) spectra of ZnO thin film annealed at 600 °C

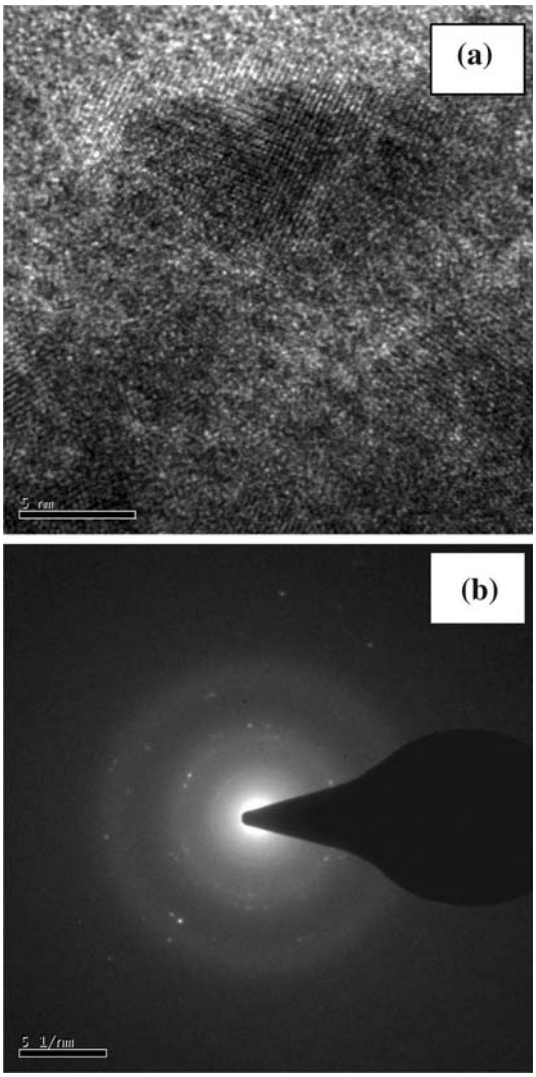

Fig. 4 **a** and **b** shows TEM image and Electron diffraction pattern of ZnO thin film annealed at 600 °C

around 10–20 nm. Figure 4b shows Electron diffraction pattern of ZnO thin film annealed at 600 °C. It shows that the ZnO films exhibited Hexagonal structure.

The film microstructure was studied using Scanning Electron Microscopy. Figure 5 shows the SEM morphology of ZnO thin film annealed at different temperatures 450–600 °C. The films consist in nanocrystalline grains randomly distributed with voids in different regions [17, 18]. The grain size increased with increasing heating temperature. The thickness of the film was confirmed from cross sectional view of SEM and it is in the range of 90–110 nm per coat using our solution and deposition parameters

3.3 Electrical conduction studies

The dc conductivity σ_{dc} of ZnO film as a function of reciprocal temperature measured at different dc bias is shown in Fig. 6. The dc conductivity was found to be in the range of 10^{-5}–10^{-6} $(\Omega\ \mathrm{cm})^{-1}$.

The temperature dependence of the dc conductivity is given as;

$$\sigma_{dc} = \sigma_0 \exp(-\delta E/k_B T). \quad (1)$$

where δE is the activation energy and is k_B Boltzman constant.

3.4 Optical studies

3.4.1 Absorption edge

Figure 7 shows optical transmittance spectra of ZnO thin film in the wavelength (λ) range 300–1,000 nm for the ZnO films formed by the spin-coating method at different annealing temperatures. The optical spectra for all samples give the transparency in the visible range above $\lambda = 400$ nm. Sharp ultraviolet absorption edges at approximately $\lambda = 390$ nm are observed, depending on the annealing temperature.

The absorption coefficient α (ω) (ω is angular frequency) is given by the transmittance T and film thickness d using the formula [19, 20],

$$\alpha(\omega) = 2.303 \log_{10}(1/T)/d. \quad (2)$$

When α (ω) exceeds 10^4 cm^{-1}, α obeys the relationship as [19, 20],

$$\alpha(\omega) = B(\hbar\omega - E_{opt})^n/\hbar\omega, \quad (3)$$

where $\hbar\omega$ is the photon energy, E_{opt} the optical band gap energy, and B is a constant having a value between 10^5 and 10^6 cm^{-1}. The exponent n takes values of 1, 2, 3, 1/2 depending on the types of electronic transition in the k-space. Using the α (ω) data calculated from Eq. 2, we

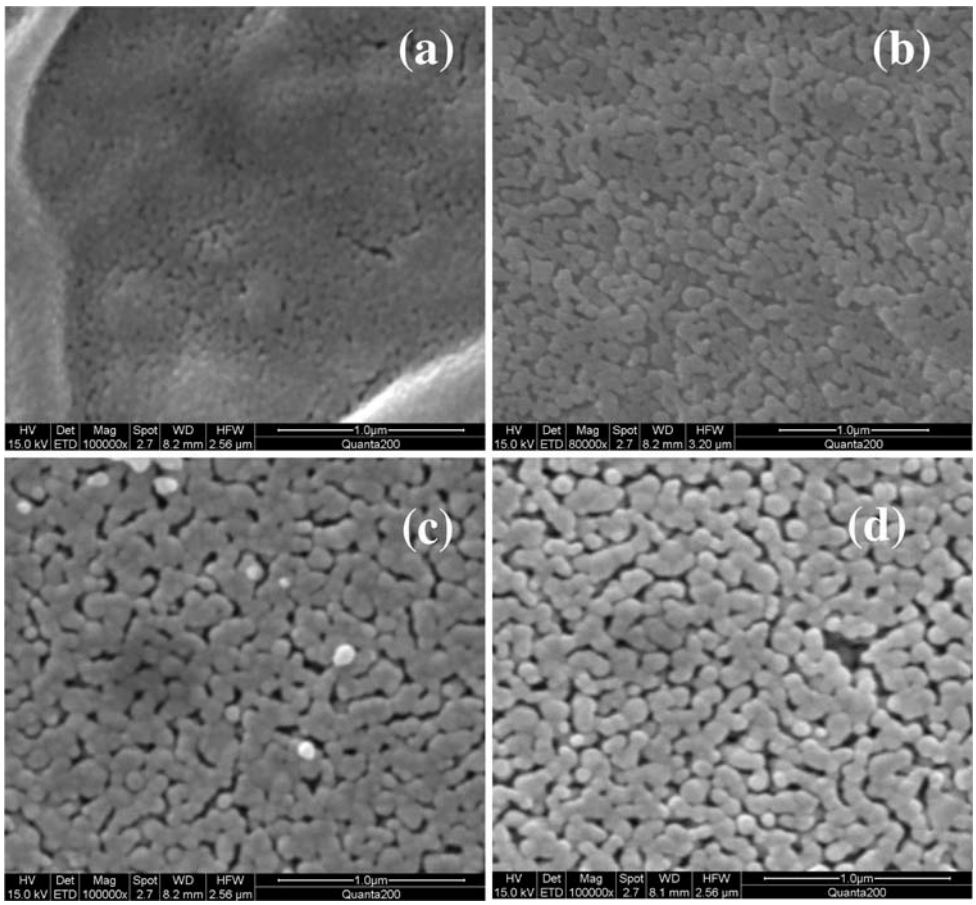

Fig. 5 SEM images of ZnO thin films at different annealing temperatures: **a** 400 °C, **b** 500 °C, **c** 550 °C and **d** 600 °C

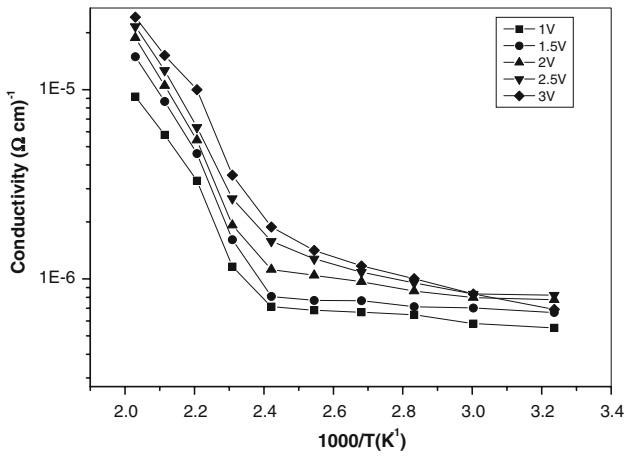

Fig. 6 Arrhenius plot of DC conductivity versus 1,000/T of ZnO thin film grown at 600 °C for different voltages

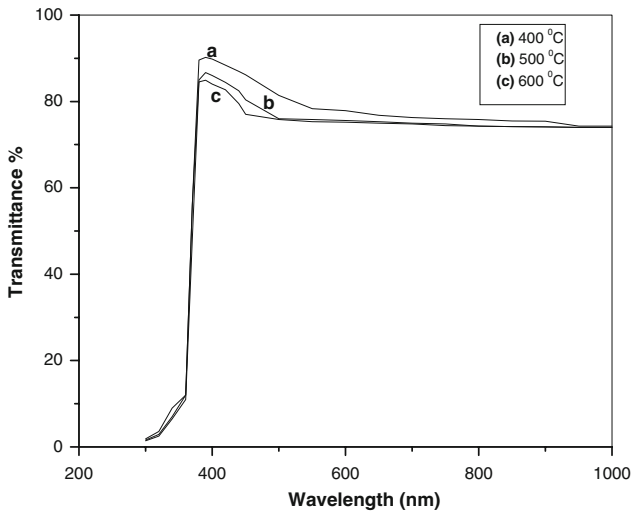

Fig. 7 Optical transmittance spectrum of ZnO thin films for different annealing temperatures

estimated E_{opt} for wavelengths shorter than 400 nm. The plot of $\alpha\hbar\omega$ versus $\hbar\omega$ shows a good linearity and therefore n predicted to be equal to 1. Here E_{opt} and B values are listed in Table 1. The E_{opt} values in Table 1 give $E_{opt} = 3.20$–3.21 eV, indicate that electronic transitions are of direct type.

3.4.2 *Exponential absorption tail*

The absorption coefficient α (ω) in the low energy range follows the well-known exponential law, that is, the Urbach tail expressed by [19, 20],

Table 1 Optical parameters of ZnO films

Sr. no.	Annealing temperature (°C)	Film thickness (nm)	E_{opt} (eV)	E_σ (eV)	B (10^6 cm^{-1})
1	450	115	3.21	0.08	2.05
2	500	126	3.20	0.08	1.57
3	550	140	3.20	0.07	1.76
4	600	150	3.20	0.08	2.17

$$\alpha(\omega) = \alpha_0 \exp(\hbar\omega/E_\sigma). \quad (4)$$

where, α_0 is a constant, E_σ denotes an energy which is constant or weakly dependent on temperature and is often interpreted as the width of the tail of localized states in the band gap.

E_σ values were estimated from the slopes of the linear relationship ln α against $\hbar\omega$ using Eq. 4. E_σ values, as given in Table 1. Therefore, the present films have many localized states originating from the donor levels due to the interstitial Zn atoms. This supports the nearest neighbor hopping transport in the present zinc oxide film.

4 Conclusions

The present work involved study of Zinc Oxide thin films by sol–gel spin coating deposition techniques for growth of high quality ZnO thin films. The ZnO has been crystallized in a hexagonal wrutzite form. The energy-dispersive X-ray (EDX) spectrometry shows Zn and O elements in the products with an approximate molar ratio. TEM image of ZnO thin shows that a grain of about 60–80 nm in size is really aggregate of many small crystallites of around 10–20 nm. Electron diffraction pattern shows that the ZnO films exhibited Hexagonal structure.

The dc conductivity found in the range of 10^{-5}–10^{-6} $(\Omega\ cm)^{-1}$.

The optical study showed that the spectra for all samples give the transparency in the visible range.

Acknowledgments One of the authors (VBP) thankful to Indian Academy of Sciences, Bangalore for awarding Summer Research Fellowship. Thanks are due to all Materials Research Centre, Indian Institute of Science, Bangalore providing the necessary support. Thanks are also extended to Nanocentre, Indian Institute of Science for providing EDX and TEM facility.

References

1. F.C.M. Van De Pol, Ceram. Bull. **69**, 1959 (1990)
2. E.L. Paradis, A.J. Shucks, Thin Solid Films **38**, 131 (1976). doi:10.1016/0040-6090(76)90220-0
3. M. Hiramatsu, K. Imaeda, N. Horio, M. Nawata, J. Vac. Sci. Technol. **A16**, 669 (1998)
4. D.S. King, R.M. Nix, J. Catal. **160**, 76 (1996)
5. Y. Chen, D.M. Bagnall, H. Koh, K. Park, K. Hiraga, Z. Zhu, T. Yao, J. Appl. Phys. **84**, 3912 (1998)
6. J.B. Webb, D.F. Williams, M. Buchanan, Appl. Phys. Lett. **39**, 640 (1981)
7. M.J. Brett, R.W. McMahon, J. Affinito, R.R. Parsons, J. Vac.Sci. Technol. **A1**, 352 (1983)
8. T. Minami, H. Nanto, S. Takata, Thin Solid Films **124**, 43 (1985)
9. J.A. Aranovich, D. Golmayo, A.L. Fahrenbruch, R.H. Bube, J. Appl. Phys. **51**, 4260 (1980)
10. Z.-C. Jin, I. Hamberg, C.G. Granqvist, B.E. Sernelius, K.-F. Berggrem, Thin Solid Films **164**, 381 (1988)
11. S. Pizzini, N. Butta, D. Narducci, M. Palladino, J. Electrochem. Soc. **136**, 1945 (1989)
12. G.S. Kino, R.S. Wagers, J. Appl. Phys. **44**, 1480 (1973)
13. T. Hata, T. Minamikawa, O. Morimoto, T. Hada, J. Cryst. Growth **47**, 171 (1979)
14. K.B. Sundaram, A. Khan, Thin Solid Films **295**, 87 (1997)
15. J. Aranovich, A. Ortiz, R.H. Bube, J. Vac. Sci. Technol. **16**, 994 (1979)
16. M.N. Islam, M.O. Hakim, H. Rahman, J. Mater. Sci. **22**, 1379 (1987)
17. S. Major, K.L. Chopra, Sol. Energy Mater. **17**, 319 (1988)
18. M.L. de la Olvera, A. Maldonado, R. Asomoza, M. Konagai, M. Asomoza, Thin Solid Films **229**, 196 (1993)
19. S.K. Ghandhi, R.J. Field, J.R. Shealy, Appl. Phys. Lett. **37**, 449 (1980)
20. A.P. Roth, D.F. Williams, J. Appl. Phys. **52**, 6685 (1981)
21. K. Kamata, S. Matsumoto, J. Ceram, Soc. Japan **89**, 337 (1981)
22. P. Souleite, B.W. Wessels, J. Mater. Res. **3**, 740 (1988)
23. Y. Natsume, H. Sakata, T. Hirayama, H. Yanagida, J. Appl. Phys. **72**, 4203 (1992)
24. W. Tang, D.C. Cameron, Thin Solid Films **238**, 83 (1994)
25. V. Craciun, J. Elders, J.G.E. Gardeniers, I.W. Boyd, Appl. Phys. Lett **65**, 2963 (1994)
26. K.L. Narasimhan, S.P. Pai, V.R. Palkar, R. Pinto, Thin Solid Films. **295**, 104 (1997)